IJHSR
ijhighschoolresearch.org
RESEARCH ARTICLE

Analysis and Discussion of Solutions to the Schrödinger Equation Under a Sawtooth Potential

Zhixuan, Tao

Westlake Boys High School, 30 Forrest Hill Road, Forrest Hill, Auckland, 0620, New Zealand; jason.tao.personal@gmail.com

ABSTRACT: Sawtooth potentials—piecewise-linear potentials defined by alternating rising and falling slopes—have garnered interest for their roles in classical Brownian ratchets, quantum transport, and flat bands in ultracold-atom lattices. However, a general solution of the time-independent Schrödinger equation for an arbitrary asymmetric sawtooth potential and a study of its band structure remain absent from the literature. We derive the exact analytical eigenstates in terms of Airy functions, but due to numerical difficulty, we solved for the eigenstates using a piecewise constant "staircase approximation." We find localized low-energy states confined within individual wells and plane waves for high energies. We apply the obtained solutions to investigate the relationship between bandwidth and parameters of the sawtooth potentials, which could offer design principles for realizing flatbands in condensed-matter and ultracold-atom research. We find that the bandwidth of the lowest energy band is entirely independent of the sawtooth's asymmetry, while it remains inversely correlated with potential height and cell size. The methodologies presented here provide a toolkit for further exploration of sawtooth potentials.

KEYWORDS: Physics and Astronomy, Theoretical, Computational and Quantum Physics, Solid State Physics, Sawtooth Potentials, Flat bands.

Introduction

Sawtooth potentials, characterized by a pattern of regions of increasing potential followed by regions of decreasing potential, have long been of interest across many fields. Sawtooth potentials are studied extensively in Brownian ratchet theory, where asymmetric sawtooth potentials are found to drive unidirectional transport when energy input is used to switch the potential between one of 2 states (a "flashing ratchet" that rectifies Brownian transport).[1] Such properties of the classical sawtooth potential are what drive motor proteins and many other essential intracellular transport processes.[2] Quantum mechanical treatment of sawtooth potentials also demonstrates transport phenomena. By exposing Bose-Einstein condensates to sawtooth-like optical lattices whose amplitudes are periodically modulated with time, a directed atomic current is observed despite the lack of dissipative processes.[3]

Sawtooth potentials are of interest in condensed matter physics for their ability to create flat bands.[4] A flat band is an energy band where energy is largely independent of the crystal momentum; this allows weak interactions to dominate. Flat bands are theorized to host a wealth of exotic behaviors, including high-T superconductivity, Wigner crystallization, and complex ferromagnetic behaviors.[5] Ultracold atoms in tunable optical lattices that have sawtooth characteristics have been utilized to engineer a nearly flat energy band in the sawtooth geometry.[4]

Much of the literature surrounding a quantum mechanical treatment of sawtooth potentials focuses on their ability to drive transport. A common area of study is to examine the transport properties of the sawtooth potential through the Schrödinger equation.[3-7] The exact solution to an asymmetric V-shaped potential has been used to investigate how the asymmetry of a sawtooth potential could affect tunneling probabilities and thus the transport properties of the sawtooth potential,[6] but the solutions to the Schrödinger equation for the sawtooth potential were never obtained. We will, in this paper, instead focus on obtaining solutions to the time-independent Schrödinger equation under a sawtooth potential, and examining its band structure, neither of which has been done for a generally applicable case in the literature. We hope the methods introduced in this paper will help others research into the theory behind the sawtooth potential, and that the findings may offer insight into design principles for flat bands.

Methods

Defining variables:

We first define the sawtooth potential by the following constants (Figure 1). We consider a single sawtooth to be a section of increasing potential, followed by a section of decreasing potential. Let $V_{\mathbf{top}}$ be the height of the potential at the tip of the sawtooth. Let the slope of the increasing side of the sawtooth be k_1 and the decreasing side by k_2. By definition, $k_1 > 0$ and $k_2 < 0$. The total width T of a sawtooth will then be $\frac{V_{top}}{k_1} - \frac{V_{top}}{k_2}$. The asymmetry ξ of a sawtooth potential will be given by the fraction of the sawtooth across which the potential is rising, given by the following $\xi = \frac{k_2}{k_2 - k_1}$, with $0 < \xi < 1$.

DOI: 10.36838/v8i2.7

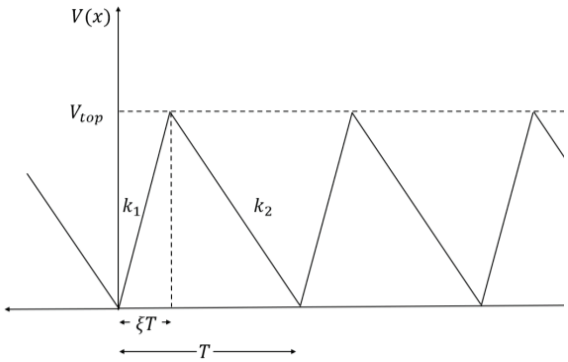

Figure 1: The parameters for our sawtooth potential. Across a singular sawtooth of size T, the potential increases linearly to V_{top} over a distance ξT, then decreases linearly to 0 over a distance $(1-\xi)T$.

The eigenstates for a singular sawtooth:

Let's examine the rising potential side with slope k_1. This gives the potential function V(x) = k_1x. Plugging into the time-independent Schrödinger equation, we arrive at

$$\frac{\hbar^2}{2m}\frac{d^2}{dx^2}\psi(x) + xk_1\psi(x) = E\psi(x) \tag{1}$$

$$\frac{\hbar^2}{2m}\frac{d^2}{dx^2}\psi(x) + (xk_1 - E)\psi(x) = 0 \tag{2}$$

This differential equation is close to the form $\boldsymbol{y''+xy=0}$, whose solution is known to be a linear combination of Airy functions.[8] Our aim now will be to express the above differential equation in the form of $\boldsymbol{y''+xy=0}$. We first define a new variable $\boldsymbol{z_n} = \left(\frac{2mk_n}{\hbar^2}\right)^{1/3}\left(x - \frac{E}{k_n}\right)$. For simplicity's sake, we will define a constant $\boldsymbol{a_n} = \left(\frac{2mk_n}{\hbar^2}\right)^{1/3}$. Note that our potential will still be defined in terms of x. Rewriting the TISE in this variable with n=1, we arrive at the following.

$$z_1 = \mathrm{a}_1\left(x - \frac{E}{k_1}\right) \tag{3}$$

$$\frac{\hbar^2}{2m}\frac{d^2}{dx^2}\psi(z_1) + \frac{k_1 z_1}{a_1}\psi(z_1) = 0 \tag{4}$$

Applying the chain rule and the fact that $\boldsymbol{z_n}$ is linear in $\boldsymbol{x}$, we arrive at

$$\frac{d^2}{dx^2}\psi(z_1) = \left(\frac{dz_1}{dx}\right)^2\frac{d^2}{dz_1^2}\psi(z_1) = a_1^2\frac{d^2}{dz_1^2}\psi(z_1) \tag{5}$$

and as $\boldsymbol{a^3/k_1=2m/\hbar^2}$,

$$\frac{d^2}{dz_1^2}\psi(z_1) + z_1\psi(z_1) = 0 \tag{6}$$

The time-independent Schrodinger equation has been reduced to the form $\boldsymbol{y''+xy=0}$, as shown above, the solution to which is shown below. $\mathbf{C_{A,1}}$ and $\mathbf{C_{B,1}}$ are arbitrary constants, where the number subscript denotes the value of n, and the letter denotes whether its Ai(x) or Bi(x).

$$\psi(z_1) = C_{A,1}Ai(z_1) + C_{B,1}Bi(z_1) \tag{7}$$

Given that $\mathbf{Bi(}\boldsymbol{x}\mathbf{)}$ diverges as $\boldsymbol{x\to\infty}$ (Figure 2), $\mathbf{C_{B,1}=0}$, as otherwise the wavefunction will not be normalizable: $\boldsymbol{\psi(x)}$ must vanish as $\boldsymbol{x\to\pm\infty}$. By plugging in $\boldsymbol{k_2}$, we obtain the wavefunction for the 2 sides of the sawtooth. Furthermore, the wavefunction and its derivative must be continuous such that the second derivative of the wavefunction present in the TISE is defined. Hence, we enforce the following boundary conditions at $\boldsymbol{x=0}$.

$$C_{A,1}\mathrm{Ai}(-a_1E/k_1) = C_{A,2}\mathrm{Ai}(-a_2E/k_2) \tag{8}$$

$$\frac{C_{A,1}}{C_{A,2}} = \frac{\mathrm{Ai}(-a_2E/k_2)}{\mathrm{Ai}(-a_1E/k_1)} \tag{9}$$

(continuity of the wavefunction)

$$\frac{C_{A,1}}{C_{A,2}} = \frac{a_2\mathrm{Ai}'(-a_2E/k_2)}{a_1\mathrm{Ai}'(-a_1E/k_1)} \tag{10}$$

(continuity of the derivative)

This set of boundary conditions allows us to solve for the values of En in the spectrum of the wavefunction. However, given the non-elementary expression of the Airy functions, solving for the spectrum will need to be done numerically.

$$\psi(x)_n = \begin{cases} C_{A,2}\mathrm{Ai}(a_2(x - \frac{E_n}{k_2})) & x \le 0 \\ C_{A,1}\mathrm{Ai}(a_1(x - \frac{E_n}{k_1})) & x \ge 0 \end{cases} \tag{11}$$

Normalization of a single sawtooth and solving for the exact values of $\boldsymbol{C}$ in this way can be done numerically. However, as the goal is to extrapolate this solution to an infinite periodic sawtooth potential, which is not normalizable over all $\mathbf{x}$, we do not discuss these results further.

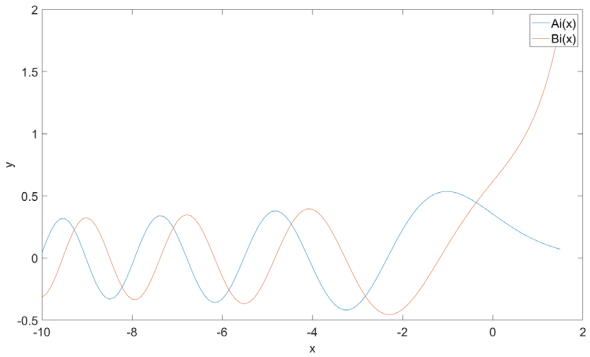

Figure 2: Ai(x) and Bi(x). Note Bi(x)'s divergence with increasing x.

The infinite periodic sawtooth potential:

When extrapolating our results from the previous section to an infinite periodic sawtooth, we may include $\mathbf{Bi(}\boldsymbol{x}\mathbf{)}$ terms as the function is never allowed to diverge to infinity, as each length of the slopes in a sawtooth is finite. In the unit cell at the origin, on the increasing slopes, we have the following wave function.

$$\psi_1(z_1) = C_{A,1}Ai(z_1) + C_{B,1}Bi(z_1) \tag{12}$$

And on the decreasing slopes, the wavefunction is

$$\psi_2(z_2) = C_{A,2}Ai(z_2) + C_{B,2}Bi(z_2) \tag{13}$$

Where $C_{A,1}$, $C_{B,1}$, $C_{A,2}$, and $C_{B,2}$ are constants to be determined through boundary conditions and subsequent normalization. A reminder that $z_n=\left(\frac{2mk_n}{\hbar^2}\right)^{1/3}\left(x-\frac{E}{k_n}\right)$ and $a_n=\left(\frac{2mk_n}{\hbar^2}\right)^{1/3}$. The boundary conditions at x=0 are as follows

$$C_{A,1}\mathrm{Ai}(-a_1E/k_1) + C_{B,1}\mathrm{Bi}(-a_1E/k_1) = C_{A,2}\mathrm{Ai}(-a_2E/k_2) + C_{B,2}\mathrm{Bi}(-a_2E/k_2) \tag{14}$$

$$a_1C_{A,1}\mathrm{Ai}'(-a_1E/k_1) + a_1C_{B,1}\mathrm{Bi}'(-a_1E/k_1) = a_2C_{A,2}\mathrm{Ai}'(-a_2E/k_2) + a_2C_{B,2}\mathrm{Bi}'(-a_2E/k_2) \tag{15}$$

When employing boundary conditions for the points where 2 unit cells meet, we must apply Bloch's theorem, which states that solutions to the Schrödinger equation in a periodic potential can be expressed as plane waves modulated by periodic functions.[9] Essentially, for periodic potentials that span the entire x-axis, due to the translational symmetry of $|\psi(x)|^2$, unit cells of the overall wavefunction may only differ by a phase e^{ikT} where T is the length of one unit cell.

$$\psi(x+T) = e^{ikT}\psi(x) \tag{16}$$

This can be expressed as a boundary condition on our wavefunction and is given below.

$$C_{A,1}\mathrm{Ai}(a_1(\frac{V_{top}}{k_1}-\frac{E}{k_1})) + C_{B,1}\mathrm{Bi}(\frac{V_{top}}{k_1}-\frac{E}{k_1}) = e^{ikT}(C_{A,2}\mathrm{Ai}(\frac{V_{top}}{k_2}-\frac{E}{k_2}) + C_{B,2}\mathrm{Bi}(\frac{V_{top}}{k_2}-\frac{E}{k_2})) \tag{17}$$

$$C_{A,1}a_1\mathrm{Ai}'(a_1(\frac{V_{top}}{k_1}-\frac{E}{k_1})) + C_{B,1}a_1\mathrm{Bi}'(a_1(\frac{V_{top}}{k_1}-\frac{E}{k_1})) \quad e^{ikT}(C_{A,2}a_2\mathrm{Ai}(a_1(\frac{V_{top}}{k_2}-\frac{E}{k_2})) + C_{B,2}a_2\mathrm{Bi}(a_2(\frac{V_{top}}{k_2}-\frac{E}{k_2})) \tag{18}$$

We apply this to our wavefunction at points where $V(x)=V_{top}$. We note that this set of boundary conditions, after rearranging for 0, is a homogeneous system of linear equations where the variables are $C_{A,1}$, $C_{B,1}$, $C_{A,2}$, and $C_{B,2}$,. For such systems, there is either only a trivial solution ($C_{A,1}=C_{B,1}=C_{A,2}=C_{B,2}=0$) or an infinite number of solutions, of which we are only interested in the latter. By rearranging Eq. 14-18 for 0, We express this system of equations in matrix form, where **M** represents the coefficient matrix for the aforementioned variables.

$$M=\begin{bmatrix} \mathrm{Ai}(\alpha) & \mathrm{Bi}(\alpha) & -\mathrm{Ai}(\beta) & -\mathrm{Bi}(\beta) \\ a_1\mathrm{Ai}'(\alpha) & a_1\mathrm{Bi}'(\alpha) & -a_2\mathrm{Ai}'(\beta) & -a_2\mathrm{Bi}'(\beta) \\ \mathrm{Ai}(\gamma) & \mathrm{Bi}(\gamma) & -e^{ikT}\mathrm{Ai}(\delta) & -e^{ikT}\mathrm{Bi}(\delta) \\ a_1\mathrm{Ai}'(\gamma) & a_1\mathrm{Bi}'(\gamma) & -e^{ikT}a_2\mathrm{Ai}'(\delta) & -e^{ikT}a_2\mathrm{Bi}'(\delta) \end{bmatrix}\begin{bmatrix} C_{A,1} \\ C_{B,1} \\ C_{A,2} \\ C_{B,2} \end{bmatrix} = \begin{bmatrix} 0 \\ 0 \\ 0 \\ 0 \end{bmatrix}$$

$$\begin{aligned} \alpha &= -\frac{a_1E}{k_1} \\ \beta &= -\frac{a_2E}{k_2} \\ \gamma &= a_1\left(\frac{V_{top}}{k_1}-\frac{E}{k_1}\right) = \frac{a_1(V_{top}-E)}{k_1} \\ \delta &= a_2\left(\frac{V_{top}}{k_2}-\frac{E}{k_2}\right) = \frac{a_2(V_{top}-E)}{k_2} \end{aligned} \tag{19}$$

The condition for an infinite number of solutions reduces to **det(M) = 0**; we solve for the null space of **M**.[10] The free variable we are left with can then be determined by normalization.

An approximation:

An exact solution for $C_{A,1}$, $C_{B,1}$, $C_{A,2}$, $C_{B,2}$ and E is difficult due to the many transcendental elements present inside **M**. However, we can approximately solve for this potential by using an approximation. We employ a piecewise-constant approximation for our sawtooth potential. We discretize our potential into N equal-length "slices" of a constant potential (Figure 3). The value of the constant potential is the midpoint of the potential between the endpoints of the slice. The solution to this "staircase potential" asymptotically approaches the solution of the exact sawtooth potential as $N \to \infty$. The oscillatory solutions to the Schrodinger equation for a constant potential are numerically more stable when one imposes boundary conditions: Airy

$$\frac{\hbar^2}{2m}\frac{d^2}{dx^2}\psi_n(x) + (V_n - E)\psi_n(x) = 0 \tag{20}$$

$$\frac{d^2}{dx^2}\psi_n(x) + \frac{2m(V_n-E)}{\hbar^2}\psi_n(x) = 0 \tag{21}$$

$$\kappa_n = \sqrt{\frac{2m(V_n-E)}{\hbar^2}} \quad \psi_n(x) = e^{\pm\kappa_n x} \tag{22}$$

$$\psi_n(x) = P_1\cos\big(\kappa_n(x-n\Delta x)\big) + P_2\sin\big(\kappa_n(x-n\Delta x)\big) \tag{23}$$

$$\psi_n'(x) = P_1\kappa_n\cos\big(\kappa_n(x-n\Delta x)\big) - P_2\kappa_n\sin\big(\kappa_n(x-n\Delta x)\big) \tag{24}$$

functions are oscillatory for $x < 0$ and then rapidly decaying/growing for $x > 0$ (Figure 2).

Here we represent the exponential solutions in a trigonometric basis (though for energies greater than the potential, they are hyperbolic as κ becomes imaginary). To determine the constants P_1 and P_2, we employ a transfer matrix method.[11] The transfer matrix **Q** that propagates across one of the slices is as follows.

DOI: 10.36838/v8i2.7

$$\begin{pmatrix}\psi_n(x+\Delta x)\\ \psi_n'(x+\Delta x)\end{pmatrix} = Q_n(x+\Delta x, x)\begin{pmatrix}\psi_n(x)\\ \psi_n'(x)\end{pmatrix} \tag{25}$$

$$Q_n(x+\Delta x, x) = \begin{pmatrix}\cos(\kappa_n(x-x_0)) & \frac{1}{\kappa_n}\sin(\kappa_n(x-x_0))\\ -\kappa_n\sin(\kappa_n(x-x_0)) & \cos(\kappa_n(x-x_0))\end{pmatrix} \tag{26}$$

We then multiply all transfer matrices for N slices to get the overall transfer matrix for one unit cell, $\mathbf{Q_{total}}$. In this paper, N **= 500** was used. Enforcing the Bloch boundary conditions returns an eigenvalue equation for the total transfer matrix that then defines the allowed energies E and the dispersion relationship.[11] This can further be simplified to an equation in terms of $\mathbf{Tr(Q_{total})}$.

$$\mathrm{Tr}\ (Q_{total}) = 2\cos(kT) \tag{27}$$

This equation was solved numerically using a root-finder algorithm in MATLAB. Reconstructing the wave function afterwards is straightforward. Note that one needs to choose the initial values for $\psi(x)$ and $\psi'(x)$ at some arbitrary x. However, because of the arbitrariness of the overall phase for the wavefunction and the subsequent unit cell normalization we perform, the exact initial choice does not matter so long as the initial transfer matrix is not singular.

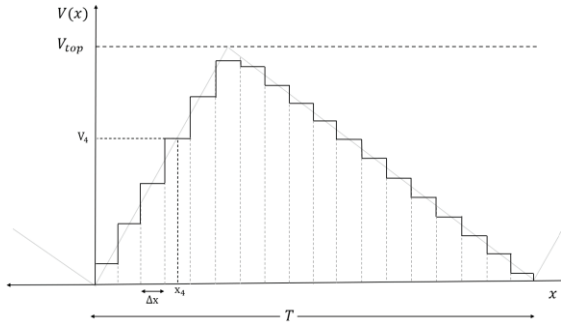

Figure 3: The staircase potential. N=18 was used here for effect: N=500 is used for actual results. The potential of the 4th slice V_4 is taken as the potential of the exact sawtooth potential at the midpoint of the slice x_4.

Result and Discussion

We used a piecewise constant approximation to obtain the band structure for a sawtooth potential of arbitrary asymmetry ξ, height V_{top}, rising slope k_1, and falling slope k_2 (Figure 4). From this, we reconstructed the solutions to the time-independent Schrodinger equation under a sawtooth potential. Throughout all visualizations from here, we have taken mass to be the mass of an electron (m **= 9.11x10^{-31} kg**). The band structures were visualized up to the first Brillouin zone for $0 \le k \le \pi/T$ sufficient to capture all the unique states due to the periodicity of the Bloch phase.

We will now examine the wavefunction and the band structure for ξ **= 0.3**, V_{top} **= 0.3eV**, and T **= 1nm**. Low energy solutions ($E < V_{top}$) are localized within each well of the sawtooth (Figure 5). The general profile of the wave function did not change significantly with energy for lower energies. In the low-energy regime, the probability density peaks at the lowest point of the sawtooth potential and dips throughout the sawtooth itself, demonstrating significant localization. When $E > V_{top}$, the solutions (Figure 6 and Figure 7) resemble plane waves with some periodic modulations, as one would expect. Our methodology allows us to freely change the ξ (Figure 8).

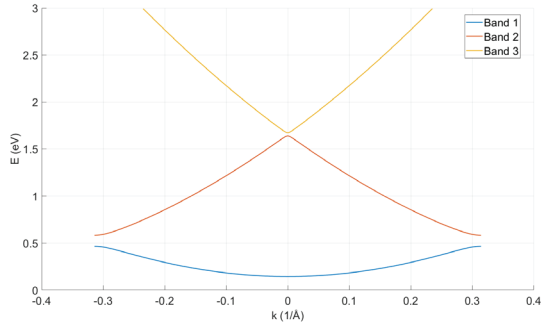

Figure 4: The band structure for ξ **= 0.3**, V_{top} **= 0.3eV**, and T **= 1nm**. One can see that the first band is the flattest. It will be the focus of the next analysis.

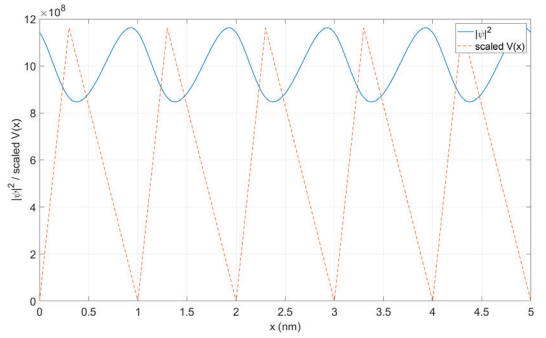

Figure 5: Probability density at E = 0.148eV for ξ **= 0.3**, V_{top} **= 0.3eV**, and T **=1nm**. The probability density has been shown in blue, and the potential is shown in orange for effect. Low-energy solutions are highly localized, as one would expect.

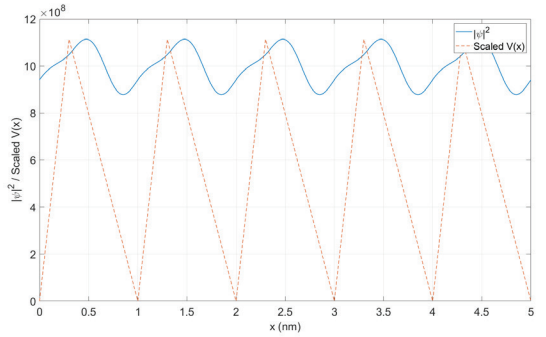

Figure 6: Probability density at E = 1.073eV for ξ **= 0.3**, V_{top} **= 0.3eV**, and T **=1nm**. As energy increases, the solutions are more reminiscent of plane waves.

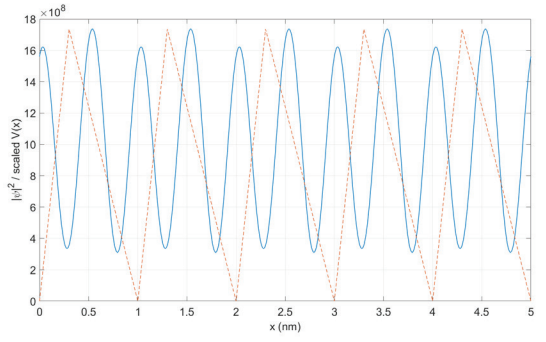

Figure 7: Probability density at E = 1.631eV for ξ **= 0.3**, V_{top} **= 0.3eV**, and T **=1nm**. At high energies, solutions resemble plane waves with periodic modulations.

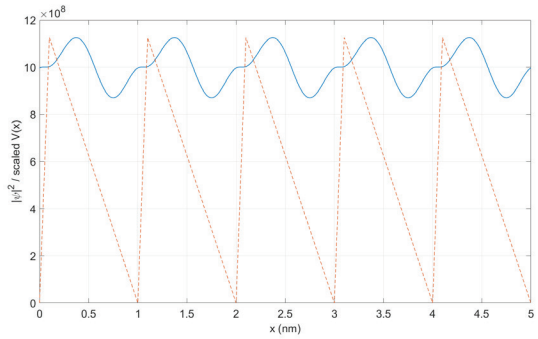

Figure 8: Probability density at E = 1.005eV for ξ **= 0.1**, V_{top} **= 0.3eV**, and T **=1nm**. Our methodology still works for more extreme values of ξ.

Asymmetry and band structure:

We mentioned before that sawtooth potentials have been studied for their ability to create "flat bands", bands of very low bandwidth (slowly varying E with $\underline{k}$) that are experimentally useful in studying weak interactions. By examining how the width of the lowest energy band varies with parameters of the lattice (V_{top} , ξ, and T), we better understand under what conditions flat bands are observed in sawtooth potentials.

We find no dependence of the bandwidth on ξ at a constant V_{top} **= 0.3eV**, and T**=1nm** (Figure 8). This is quite an interesting result, but we can motivate it through a semi-classical treatment of the potential. The tunneling amplitude through a singular sawtooth, and thus bandwidth, is dependent on the integral of the square root of V(x) over the classically forbidden region for a singular sawtooth.[12,13] The classically forbidden region for a particle with $E < V_{top}$ is given by $V_{top}/k_2 \le x \le E/k_2$ and $E/k_1 \le x \le V_{top}/k_1$. The WKB action over the region is then given by

$$S_L = \int_{V_{top}/k_2}^{E/k_2} \sqrt{2m\,(k_2\,x - E)}\,dx = -\frac{2\sqrt{2m}}{3k_2}\,(V_{top} - E)^{3/2}, \qquad (27)$$

$$S_R = \int_{E/k_1}^{V_{top}/k_1} \sqrt{2m\,(k_1\,x - E)}\,dx = \frac{2\sqrt{2m}}{3\,k_1}\,(V_{top} - E)^{3/2}. \qquad (28)$$

$$S = S_L + S_R = \frac{2\sqrt{2m}}{3}(V_{top} - E)^{3/2}\left(\frac{1}{k_1} - \frac{1}{k_2}\right) \qquad (29)$$

Since $T = \frac{V_{top}}{k_1} - \frac{V_{top}}{k_2}$, without changing T, the WKB action and thus the tunneling amplitude are not dependent on the asymmetry. Thus, we might expect the bandwidth of the first band not to depend on asymmetry ξ. This is unique to the sawtooth potential: a general skewing of a potential function that leaves the area under the function unchanged would not leave the WKB action unchanged due to the square root in the WKB integral. When altering ξ, one side becomes steeper but shorter, and the other becomes less steep but longer. The 2 effects happen to compensate perfectly in the case of linear functions so that the overall "tunneling difficulty" is unchanged.

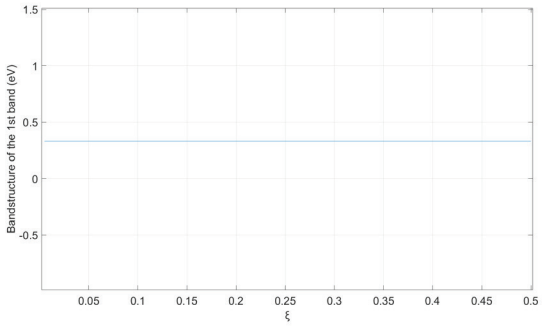

Figure 9: Bandwidth of first band (eV) vs ξ for V_{top} **= 0.3eV**, and T **= 1nm**. Bandwidth is not affected by ξ as rationalized through a semiclassical approach.

***V_{top}*, T, and band structure:**

The effect of potential height V_{top} and cell length T on band structure for a general periodic potential is well documented.[13] We will briefly present the effects of these parameters as applied to the sawtooth potential. We find that there is a strong correlation between the V_{top} and the bandwidth of the 1st band. As V_{top} increases, the tunneling amplitude across the unit cell decreases, and the bandwidth of the first band decreases (Figure 9). Similarly, as T increases, the tunneling amplitude decreases, thus decreasing the bandwidth of the 1st band (Figure 10).

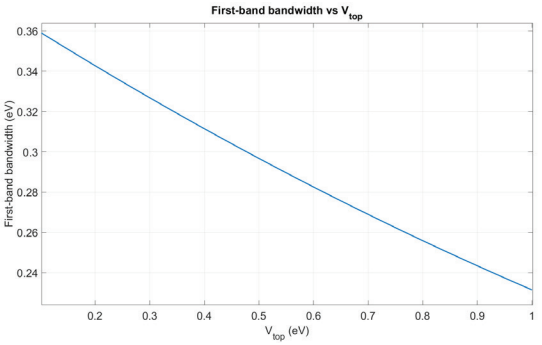

Figure 10: Bandwidth of first band (eV) vs V_{top} (eV) for ξ **= 0.3**, T **= 1nm**. Bandwidth decreases with V_{top}, as one would expect.

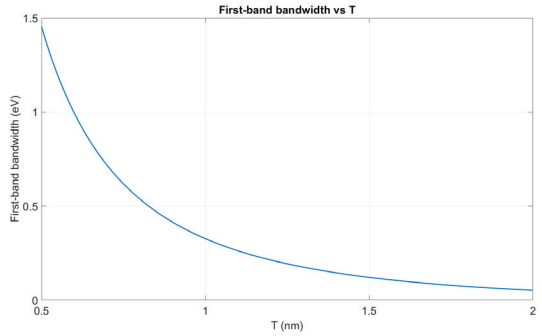

Figure 11: Bandwidth of first band (eV) vs T (nm) for V_{top} **= 0.3eV**, T **= 1nm**. Bandwidth decreases with T, as one would expect.

Conclusion

The solutions to the time-independent Schrodinger equation for a sawtooth potential were presented and visualized. We applied the solutions and the band structure to investi-

DOI: 10.36838/v8i2.7

gate the relationship between the bandwidth of the first band and parameters V_{top} , ξ, and T. As is true for general periodic potentials, we found that increasing V_{top} or T decreased the bandwidth, but interestingly, that ξ had no impact on the bandwidth, which we then motivated with a semiclassical treatment of the system. These findings could offer insights into parameter choices for flat bands in sawtooth potentials, demonstrating the utility of the obtained solutions. Furthermore, being able to alter ξ without affecting the bandwidth would allow us to alter the transport properties of the sawtooth whilst retaining a flat band and amplifying weak interactions.[3-5] Next steps could include solving numerically using Airy functions instead of using a piecewise constant approximation to provide more accurate solutions. Further research could be conducted on irregular sawtooth potentials with individual sawtooth potentials of varying shapes and sizes.

Acknowledgments

Thanks to my mentor, Adam Almakroudi, for mentoring me throughout the research process and teaching me much of the pre-requisite knowledge required.

References

1. Ait-Haddou, R.; Herzog, W. Brownian Ratchet Models of Molecular Motors. Cell Biochemistry and Biophysics 2003, 38 (2), 191–214. https://doi.org/10.1385/cbb:38:2:191.
2. Hwang, W.; Karplus, M. Structural Basis for Power Stroke vs. Brownian Ratchet Mechanisms of Motor Proteins. Proceedings of the National Academy of Sciences of the United States of America 2019, 116 (40), 19777–19785. https://doi.org/10.1073/pnas.1818589116.
3. Salger, T.; Kling, S.; Hecking, T.; Geckeler, C.; Morales-Molina, L.; Weitz, M. Directed Transport of Atoms in a Hamiltonian Quantum Ratchet. *Science (New York, N.Y.)* 2009, 326 (5957), 1241–1243. https://doi.org/10.1126/science.1179546.
4. Zhang, T.; Jo, G.-B. One-Dimensional Sawtooth and Zigzag Lattices for Ultracold Atoms. Scientific Reports 2015, 5 (1). https://doi.org/10.1038/srep16044.
5. Pyykkönen, V.; Peotta, S.; Fabritius, P.; Mohan, J.; Esslinger, T.; Törmä; Törmä, P. ETH Library Flat-Band Transport and Josephson Effect through a Finite-Size Sawtooth Lattice Flat Band Transport and Josephson Effect through a Finite-Size Sawtooth Lattice. *Physical Review B 103* (14)
6. Hodžić, M.; Ulrich, M.; Graz, H. Numerical Simulation of Directed Quantum Tunnelling; 2021. https://static.uni-graz.at/fileadmin/_Persoenliche_Webseite/hohenester_ulrich/diplomahodzic21.pdf
7. Rozenbaum, V. M.; Shapochkina, I. V.; Trakhtenberg, L. I. Quantum Particle in a V-Shaped Well of Arbitrary Asymmetry. Brownian Motors. Physics-Uspekhi 2024, 67 (10), 1046–1055. https://doi.org/10.3367/ufne.2024.06.039704.
8. Vallée, O., & Soares, M. (2004). Airy Functions and Applications to Physics. IMPERIAL COLLEGE PRESS. https://doi.org/10.1142/p345
9. Kittel, C. Introduction to Solid State Physics, 8th ed.; Wiley: Hoboken, NJ, 2004; Chapter 9, "Energy Bands in the Nearly-Free Electron Model," Section 9.1, "Bloch Waves."
10. Strang, G. *Introduction to Linear Algebra*, 5th ed.; Wellesley–Cambridge Press: Wellesley, MA, 2016; Chapter 3, "Solving Ax = 0.
11. Almeida, J.; Rodrigues, T.; Bruno-Alfonso, A. Solving the Schrödinger Equation by the Transfer-Matrix Method. *Matemática Contemporânea* 2024, 59 (8). https://doi.org/10.21711/231766362024/rmc598.
12. Griffiths, D. J. *Introduction to Quantum Mechanics*, 3rd ed.; Cambridge University Press: Cambridge, UK, 2018; Chapter 11.
13. *Band structure, David Tong: Solid State Physics*. www.damtp.cam.ac.uk. https://www.damtp.cam.ac.uk/user/tong/solidstate.html.

Author

Zhixuan (Jason) Tao is an aspiring physics major based in New Zealand. Jason is interested in modern physics and, in particular, quantum mechanics, and looks forward to studying these concepts in college.